New algorithm for weak changes detection with application to real data.

Youssef Salman, Anis Hoayek, Mireille Batton-Hubert

ORIGINAL ARTICLE

New algorithm for weak changes detection with application to real data.

Youssef SALMAN[a,*], Anis HOAYEK[a] and Mireille BATTON-HUBERT[a]

[a]Mines Saint-Etienne, Univ Clermont Auvergne, CNRS, UMR 6158 LIMOS, Institut Henri Fayol, 42023, Saint-Etienne, France

ARTICLE HISTORY
Compiled October 25, 2024

ABSTRACT
In this paper, we propose a novel automatic algorithm for detecting subtle changes in the mean of piecewise stationary CHARN models. Additionally, we introduce a new technique for selecting the appropriate CHARN model to best represent the time series, taking into account the changes present in the data. Through simulation experiments, we demonstrate the algorithm's effectiveness in detecting weak changes in the mean and accurately estimating their locations. Furthermore, we validate the robustness of our algorithm by applying it to industrial data, such as welding electrical signals (WES), and financial data, including the S&P 500 and FTSE 100 Index.

KEYWORDS
CHARN model; Changepoints; Algorithm; Welding electrical signals; S&P 500; FSTE 100;

1. Introduction

A change point in a time series is a moment in time where the statistical properties of the data, such as the mean, variance, or correlation structure, undergo a significant shift. This could indicate a structural break or transition in the underlying process generating the data, such as changes in regime, seasonality, or trend. The analysis of structural change-points, or breaks, began with the work of [27] in quality control, and has since expanded into various fields, including economics [29], climatology [3, 30], finance [1], and engineering [34]. One widely used statistic for segmenting time series is the CUSUM test, introduced by [27]. [5] proposed a least-squares-based version, denoted CUSUM^{ols}. Further work by [38, 39] applied the CUSUM test to p-value estimation, addressing its low power for detecting early or late changes by updating the bounds.

Over time, many versions of the CUSUM test have been developed (see [18]). For example, [2] adapted the CUSUM approach for data with serial dependence, demonstrating how parametric modeling can recover structural breaks in the mean, variance, and second-order characteristics of time series. The literature on change points detection is extensive and covers various techniques, depending on whether data is analyzed offline or sequentially. In the offline multiple-change-point context, common approaches

CONTACT Youssef SALMAN. Email: youssef.salman@emse.fr

involve optimizing criteria like the Bayes Information Criterion (BIC) or least squares [17, 36]. However, due to the computational cost of optimization, efficient methods such as the PELT algorithm [21] and genetic algorithms [9] have been developed. Binary segmentation methods, initially proposed by [35], offer a simpler alternative to optimization-based methods.

Further advancements include the Bayesian approach by [14] for nonstationary oscillatory time series, and [8]'s binary segmentation method for detecting changes in the covariance structure of piecewise stationary time series. An important update to binary segmentation is Wild Binary Segmentation (WBS), introduced by [12] for detecting mean changes, with extensions to covariance structure detection [22].

In addition, [37] proposed a likelihood ratio scan method for estimating change points in piecewise stationary processes, utilizing local windows for computational feasibility. [15] discussed methods for detecting change points in non-exchangeable data, such as network events and financial time series, while [10] provided a Wald-type statistic for detecting distributional shifts in multivariate time series.

However, the issue of testing for weak changes in time series, where the change is of small magnitude, remains under-explored. [24] and [26] addressed this problem for the mean of Conditional Heteroscedastic Autoregressive Nonlinear (CHARN) models, with further generalization by [33]. In scenarios where changes are brief and anomalous, distinguishing between false alarms and true structural breaks is challenging. Developing techniques to address this problem is essential for accurate detection in piecewise stationary data."

The results presented in this paper are based on the theoretical results established in [33], introducing the a novel algorithm for detecting weak changes in the mean and distinguishing between false alarms and true change points by monitoring the local power of the test around the point of interest. Here, we mean by change point the change that make the data stationary by pieces. The algorithm specifically addresses the issue of white noise, which may lead to erroneous changepoint detection in the method of [33]. A portion of this work was previously published as a conference article in [32]. Here, we extend the previous work by introducing a complementary technique that identifies the optimal CHARN model to be used in conjunction with the primary automatic algorithm. Additionally, we demonstrate the enhanced performance of the method through diverse simulation experiments, which confirm the precision and efficiency of the algorithm in detecting and characterizing changes. Finally, we apply our approach to real-world industrial and financial data, with comparisons drawn against results from other research studies.

In the sequel, this paper is categorized as follows. In Section 2, we recall the essential theoretical results of [33]. These results are used in Section 3 for constructing the new algorithm. In Section 4, a simulation experiment is conducted for the application of our algorithm. In Section 5, an application to a real data set is performed. Section 6 concludes the paper.

2. Overview of the principal results from [33]

In this section, we provide a concise summary of the method developed in [33], which is a generalization of the approaches presented in [24] and [26]. These methods are designed to detect weak changes in the mean based on the theoretical power of a likelihood ratio test. The statistical model used in [33] belongs to the class of Conditional Heteroscedastic Autoregressive Nonlinear (CHARN) models (see, e.g.,

[16]).

More specifically, let $d, p, k, n \in \mathbb{N}$, with $k \ll n$. Assume that the observations $X_1, \ldots, X_n$ are generated from a piecewise stationary CHARN model.

$$X_t = T(\rho_{\mathbf{0}} + \gamma \odot \omega(t); \mathbf{X}_{t-1}) + V(\mathbf{X}_{t-1})\varepsilon_t, t \in \mathbb{Z}, \tag{1}$$

with

$$X_t = Y_{t,j} = T(\rho_{\mathbf{0}} + \boldsymbol{\gamma}_j \omega_j(t); \mathbf{X}_{t-1,j}) + V(\mathbf{X}_{t-1,j})\varepsilon_t, \quad \tau_{j-1} \leq t < \tau_j, \quad j = 1, \ldots, k+1, \tag{2}$$

where for $j = 1, \ldots, k$, $(Y_{t,j})_{t\in\mathbb{Z}}$ is a stationary and ergodic process; $\boldsymbol{\rho}_0 \in \mathbb{R}^p$, $T(\boldsymbol{\rho}_0, .)$ and $V(.)$ are real-valued functions with $\inf_{x\in\mathbb{R}^d} V(x) > 0$; the τ_j, $j = 0, \ldots, k+1$, are potential instants of changes with $\tau_0 = 1$ and $\tau_{k+1} = n+1$; for $j = 1, \ldots, k$, $\mathbf{X}_{t,j} = (Y_{t,j}, \ldots, Y_{t-d+1,j})^\top$, $\mathbf{X}_{\tau_{j-1}+\ell} = \mathbf{X}_{\tau_{j-1}+\ell,j}$, $\ell = 0, \ldots, d-1$ and for $t \in [\tau_{j-1} + d - 1, \tau_j)$, $\mathbf{X}_t = (X_t, \ldots, X_{t-d+1})^\top$; for $j, \ell = 1, \ldots, k$, $j \neq \ell$, the process $(Y_{t,j})_{t\in\mathbb{Z}}$ and $(Y_{t,\ell})_{t\in\mathbb{Z}}$ are mutually independent ([37] noted that this assumption can be extended to some weak dependence assumption); $(\varepsilon_t)_{t\in\mathbb{Z}}$ is a standard white noise with density f. $\boldsymbol{\gamma} = \left(\boldsymbol{\gamma}_1^\top, \ldots, \boldsymbol{\gamma}_{k+1}^\top\right)^\top$, $\boldsymbol{\gamma}_j \in \mathbb{R}^p$, $j = 1, \ldots, k+1$; $\omega(t) = (\mathbb{1}_{[\tau_0,\tau_1)}(t), \mathbb{1}_{[\tau_1,\tau_2)}(t), ..., \mathbb{1}_{[\tau_{k-1},\tau_k)}(t), \mathbb{1}_{[\tau_k,\tau_{k+1})}(t))^\top = (\omega_1(t), \ldots, \omega_{k+1}(t)) \in \{0,1\}^{k+1}$; for $\boldsymbol{\gamma} = (\boldsymbol{\gamma}_1^\top, \ldots, \boldsymbol{\gamma}_{k+1}^\top)^\top$ and $\omega(t) = (\omega_1(t), \ldots, \omega_{k+1}(t))^\top$, $\boldsymbol{\gamma} \odot \omega(t)$ stands for $\boldsymbol{\gamma} \odot \omega(t) = \boldsymbol{\gamma}_1\omega_1(t) + \cdots + \boldsymbol{\gamma}_{k+1}\omega_{k+1}(t) \in \mathbb{R}^p$, and $\boldsymbol{\gamma}_i\omega_i = (\gamma_{i,1}\omega_i, \ldots, \gamma_{i,p}\omega_i) \in \mathbb{R}^p$.

This category of models is expansive, encompassing a variety of models including AR(p), ARCH(p), EXPAR(p), GEXPAR(p). Statistical and probabilistic properties have been extensively investigated in the existing literature (see, e.g. [6] for the study of the ergodicity of GEXPAR models).

For $\boldsymbol{\gamma}_0 \in \mathbb{R}^{p(k+1)}$ and $\boldsymbol{\beta} \in \mathbb{R}^{p(k+1)}$ depending on the τ_j's, [33] construct a likelihood ratio test for testing

$$H_0 : \boldsymbol{\gamma} = \boldsymbol{\gamma}_0 \quad \text{against} \quad H_{\boldsymbol{\beta}}^{(n)} : \boldsymbol{\gamma} = \boldsymbol{\gamma}_n = \boldsymbol{\gamma}_0 + \frac{\boldsymbol{\beta}}{\sqrt{n}}. \tag{3}$$

Note that the norm of $\boldsymbol{\beta}$ is small in front of n, and then the two hypotheses considered are getting closer as the sample size n grows up.

First, the authors prove that the test constructed establish the locally asymptotically normal property (LAN) and the hypotheses considered are contiguous in the sens of Le Cam (see [23] and [11]). These properties allow the study of the theoretical power of the test constructed and lead to obtain an explicit expression of it. Indeed, under some technical hypotheses, they prove that the constructed likelihood ratio test is asymptotically optimal and its asymptotic power has the following expression

$$\mathcal{P}_{k,\tau^k} = 1 - \Phi(z_\alpha - \vartheta(\boldsymbol{\rho}_0, \boldsymbol{\gamma}_0, \boldsymbol{\beta})) \tag{4}$$

where

- $\boldsymbol{\rho}_0$ represent the true nuisance parameter and $\alpha \in (0,1)$ represent the level of significance,

- z_α is the $(1-\alpha)$-quantile of the standard Gaussian distribution with cumulative distribution function ϕ,
- ϑ is a real function defined in $\mathbb{R}^{p(k+1)\times p(k+1)}$, where its expression is given in [33].

In practice, the model parameters are unknown and must be estimated. Many studies focus on parameter estimation, such as [6], which discusses the estimation of both linear and non-linear components in GExpAR models, a particular case of the CHARN model studied in [33], and [4] for linear models like ARMA. In [33], a decision for the testing problem is made by estimating the test's power $\widehat{\mathcal{P}}_{k,\tau^k}$, which is obtained by substituting the true parameters with their estimators in $\mathcal{P}_{k,\tau^k}$.

To describe the estimation techniques used, for $1 \leq j \leq k+1$, $1 \leq h \leq p$, let $\widehat{\rho}_{j,h}$ be a consistent estimator (e.g., the maximum likelihood estimator) of $\rho_{0,h} + \beta_{j,h}/\sqrt{n}$ based on the observations in the interval $[\tau_{j-1}, \tau_j)$. Then, the estimator of $\beta_{j,h}$ is given by $\widehat{\beta}_{j,h} = \sqrt{n}(\widehat{\rho}_{j,h} - \widehat{\rho}_{0,h})$, where $\widehat{\rho}_{0,h}$ is the estimator of the stationary parameter $\rho_{0,h}$ based on the first segment of observations $[1, \tau_1)$. By replacing the true parameters with their estimates, it is shown that the constructed test remains asymptotically optimal, with an explicit expression for its power denoted by $\widehat{\mathcal{P}}_{k,\tau^k}$.

3. New algorithm for weak-changes detection and their locations estimation

In this section, we present two algorithms. The first is used to detect change points in time series data, and the second is for selecting the appropriate CHARN model to be used in the first algorithm, taking into account the potential unknown changes present in the data. Both approaches are explained in detail, highlighting their respective methodologies and advantages.

The algorithm introduced in [33] may be sensitive to the presence of extreme values in white noise. To illustrate this, consider two distinct time intervals, $[1, t)$ and $[t+1, n)$, where $t \in (1, n)$. Assume the parameters of the statistical model remain unchanged across both intervals, but extreme white noise values occur in one of them. In such a case, the algorithm may erroneously detect a change due to the lack of techniques to differentiate between a genuine change-point and a false alarm. As a result, the data may be incorrectly classified as piecewise stationary, with the falsely detected change marking the beginning of the next segment.
To address this issue, in SubSubsection 3.1, we introduce a new algorithm designed to reduce the impact of white noise and classify detected changes as either true change-points or false alarms.
In our study, one of the main challenges occurs during the time series modeling stage. Specifically, the challenge is determining the best approach to identify the most suitable time series model and its order, while properly addressing the potential non-stationarity present in the data.

To address our specific requirements for the second algorithm, the algorithm of [31] adjusts the CHARN model to the first m observations assumed to be stationary, then selects a suitable model to apply to the entire dataset. However, this chosen model may not remain optimal for subsequent stationary observations following any detected changes. Therefore, it is crucial to develop an algorithm that addresses this issue.

In Subsection 3.2, we propose an algorithm to resolve this problem, serving as a

preliminary step before applying the algorithm of [31]. Recall that, as stated in [31], the author assumes the presence of at least m stationary observations following each change.

3.1. Algorithm 1

Here, we retain the same notation used in [33], where $\mathcal{P}_{k,\tau^k}$ represents the theoretical power of the test at $\tau^k = (\tau_1, \ldots, \tau_k)$ for $k \geq 1$. For a significance level $\alpha \in (0,1)$, we denote $\mathcal{P}_{0,\tau^0} = \alpha$ as the nominal level of the test. Let $\zeta \in (0, 0.1)$ and $X_1, X_2, \ldots, X_m$ ($m \ll n$) be the first m stationary observations. It is important to note that, in practice, the value of m will be smaller than that considered in [33].

Our procedure for detecting weak changes in the time series $X_1, X_2, \ldots, X_n$ and estimating their locations is described in the following algorithm.

Location 1 :

Put $t = 1$

($\mathcal{S}_\mathbf{1}$) : Consider the two intervals $\mathcal{I}_1$ and $\mathcal{I}_2$ that contains respectively the observations $X_1, \ldots, X_{m+t-1}$ and $X_1, \ldots, X_{m+t}$. So that the difference between the two intervals considered is the single observation X_{m+t} which is under testing.

($\mathcal{S}_\mathbf{1}$)$'$: **Adjust** model (1) to $\mathcal{I}_1$ and $\mathcal{I}_2$. Then, apply the testing procedure presented in [33].

If $|\mathcal{P}_{1,t} - \mathcal{P}_{0,\tau^0}| > \zeta$,

Replace X_{m+t} with $X_{m+\iota}$ in $\mathcal{I}_2$, with $t+1 \leq \iota \leq j$, $j << m$, and **Repeat** ($\mathcal{S}_\mathbf{1}$)$'$ with the updated $\mathcal{I}_2$

If $|\mathcal{P}_{1,\iota} - \mathcal{P}_{0,\tau^0}| > \zeta$,

The first change location is estimated on $\tau_1 = m + t$.

Then, Go to **Location 2**.

Else

A **False Alarm** is detected.

Remove X_{m+t} from the sample, Do $t = t + 1$ and Go to ($\mathcal{S}_\mathbf{1}$).

Else

Do $t = t + 1$ and Go to ($\mathcal{S}_\mathbf{1}$).

Location 2 :

Consider the next m observations to X_{τ_1}: $X_{\tau_1+1}, \ldots, X_{\tau_1+m}$

Put $t = 1$ and Do

($\mathcal{S}_\mathbf{2}$) : Consider the two intervals $\mathcal{I}_1$ and $\mathcal{I}_2$ that contains respectively the observations $X_{\tau_1}, \ldots, X_{\tau_1+m+t-1}$ and $X_{\tau_1}, \ldots, X_{\tau_1+m+t}$. So that the difference between the two intervals considered is the single observation X_{τ_1+m+t} which is under testing.

($\mathcal{S}_\mathbf{2}$)$'$: **Adjust** model (1) to $\mathcal{I}_1$ and $\mathcal{I}_2$. Then, apply the testing procedure presented in [33].

If $|\mathcal{P}_{1,t} - \mathcal{P}_{0,\tau^0}| > \zeta$,

Replace X_{τ_1+m+t} with $X_{\tau_1+m+\iota}$ in $\mathcal{I}_2$, with $t+1 \leq \iota \leq j$, $j << m$, and **Repeat** ($\mathcal{S}_\mathbf{2}$)$'$ with the updated $\mathcal{I}_2$

If $|\mathcal{P}_{1,\iota} - \mathcal{P}_{0,\tau^0}| > \zeta$,

The second change location is estimated on $\tau_2 = \tau_1 + m + t$
Then, Go to **Location 3**.

Else
A **False Alarm** is detected.
Remove X_{τ_1+m+t} from the sample, Do $t = t + 1$ and Go to $(\mathcal{S}_\mathbf{2})$.

Else
Do $t = t + 1$ and Go to $(\mathcal{S}_\mathbf{2})$.

Location i :

We already estimated the $(i-1)^{th}$ change location τ_{i-1} in step $i-1$
Consider the next m observations to $X_{\tau_{i-1}}$: $X_{\tau_{i-1}+1}, \ldots, X_{\tau_{i-1}+m}$
Put $t = 1$ and Do
$(\mathcal{S}_\mathbf{i})$: Consider the two intervals $\mathcal{I}_1$ and $\mathcal{I}_2$ that contains respectively the observations $X_{\tau_{i-1}}, \ldots,$ $X_{\tau_{i-1}+m+t-1}$ and $X_{\tau_{i-1}}, \ldots, X_{\tau_{i-1}+m+t}$. So that the difference between the two intervals considered is the single observation under testing.
$(\mathcal{S}_\mathbf{i})'$: **Adjust** model (1) to $\mathcal{I}_1$ and $\mathcal{I}_2$. Then, apply the testing procedure presented in [33].
If $|\mathcal{P}_{1,t} - \mathcal{P}_{0,\tau^0}| > \zeta$,
Replace $X_{\tau_{i-1}+m+t}$ with $X_{\tau_{i-1}+m+\iota}$ in $\mathcal{I}_2$, with $t+1 \leq \iota \leq j$, $j << m$, and **Repeat** $(\mathcal{S}_\mathbf{i})'$ with the updated $\mathcal{I}_2$

If $|\mathcal{P}_{1,\iota} - \mathcal{P}_{0,\tau^0}| > \zeta$,
The i^{th} change location is estimated on $\tau_i = \tau_{i-1} + m + t$.
Then, Go to **Location** $i + 1$.

Else
A **False Alarm** is detected.
Remove $X_{\tau_{i-1}+m+t}$ from the sample, Do $t = t + 1$ and Go to $(\mathcal{S}_\mathbf{i})$.

Else
Do $t = t + 1$ and Go to $(\mathcal{S}_\mathbf{i})$.

3.2. Algorithm 2

Consider a set of n observations, denoted as $X_1, X_2, \ldots, X_n$. We use m as the maximum number of observations assumed to be stationary. Our additional complementary algorithm can be explained by the following steps:

(1) Consider h independent Uniform random variables $u \in U[1, n-m]$, $1 \leq h < n - m$, where m denotes the minimum number of observations assumed to be stationary as per the algorithm mentioned above:
   (a) Select a subset S_u, which contains the observations $X_{u+1}, X_{u+2}, \ldots, X_{u+m}$.
   (b) Fit the CHARN model to the time series subset S_u.
   (c) Based on different selection criteria (such as AIC, BIC, etc.), extract the best-fitting time series model that explains the behavior of the observations in S_u, denoted as M_u.
(2) The optimal model to be use for applying the algorithm described in Subsection

3.1 is:

$$M = \text{ Most frequent model } M_u \text{ among } h \text{ models}$$

4. Simulation experiment

In this section, we apply the theoretical results obtained in [33] to specifically simulated datasets using R and Python. Following the algorithms outlined in Section 3, we detect weak changes and estimate their locations. By monitoring the power of the test around each estimated change, we determine whether it represents a true change-point or a false alarm.

Initially, we analyze the power of the test to assess the occurrence of false alarms. The results demonstrate that the proposed algorithm effectively distinguishes between change-points and false alarms by examining the behavior of the power in the vicinity of detected changes. Furthermore, we evaluate the performance of our algorithm in detecting multiple weak breaks where both the number and locations of change-points are unknown. Additionally, we compare the accuracy of the estimated change locations with those obtained in [33], using the same parameter values, and find that our method provides improved precision.

For the simulation, we use the same particular CHARN model as in [33] having the following expression

$$X_t = \rho_{0,1} + \frac{\beta_{j,1}}{\sqrt{n}} + \left(\rho_{0,2} + \frac{\beta_{j,2}}{\sqrt{n}}\right) X_{t-1}\, e^{\left(\rho_{0,3}+\frac{\beta_{j,3}}{\sqrt{n}}\right) X_{t-1}^2} + \sqrt{\theta_1 + \theta_2 X_{t-1}^2}\,\varepsilon_t, \quad j = 1, \ldots, k, \quad t \in \mathbb{Z}, \tag{5}$$

where n denotes the number of observations, $(\varepsilon_t)_t$ is a standard white noise with a differentiable density f. Here, on $[\tau_{j-1}, \tau_j)$, $\boldsymbol{\rho}_0 = (\rho_{0,1}, \rho_{0,2}, \rho_{0,3}) \in \mathbb{R}^3$, $\boldsymbol{\beta}_j = (\beta_{j,1}, \beta_{j,2}, \beta_{j,3}) \in \mathbb{R}^3$; $\boldsymbol{\rho}_0$ is the parameter to be specified in each particular model considered.

4.1. Data presenting one single False Alarm

In this part, we consider the problem of detecting and identifying a change. Identifying a change means that we distinguish between a false alarm and a change-point that makes the data piece-wise stationary based on the power calculated around the estimates change.

The data are generated without any changes, meaning that using the model (5) for $\rho_{0,1} = 0.2$, $\rho_{0,2} = 0.3$ and $\rho_{0,3} = \beta_{j,1} = \beta_{j,2} = \beta_{j,3} = 0$, $j = 1, \ldots, k$, . At an instant between 1 and n, say τ_1, we replace the corresponding observation, say X_{τ_1}, by another observation, for example ϵ that follows certain distribution. . For $\zeta = 0.4\%$, $\alpha = 5\%$, $\epsilon \sim \mathcal{N}(1, 3)$ and $\tau_1 = 150$, the local power results calculated using our algorithm methodology, are depicted in Figure 1. From Figure 1, one can see that the power of the test jumps above the threshold at $t = 150$ (the threshold here is $\alpha + \zeta = 5.4\%$), which is the true instant of change, and directly it fell under the threshold for the next few observations.

For different τ_1, we monitor the power of the test calculated at $\tau_1 + i$, $i = -1, 0, \ldots, 4$. The results are shown in Table 1 and they illustrate numerically what we said about Figure 1.

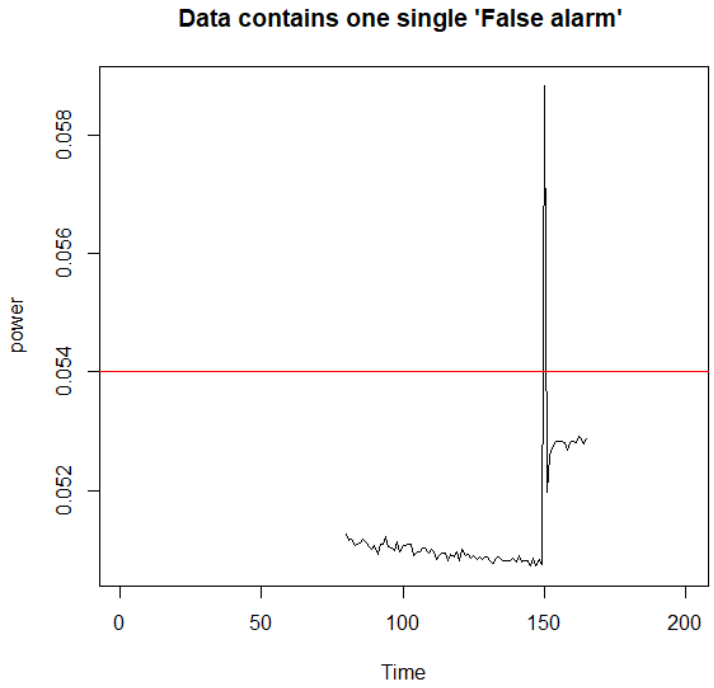

Figure 1. Estimation of the change location for $\tau_1 = 150$ in a class of AR(1) models.

One can observe that the power calculated at $\tau_1 + i$ for $i = 1, 2, 3, 4$ is higher than the values before τ_1. This is expected because these calculations were performed by removing the intermediate observation at the estimates τ_1, which affects the estimation of possible autocorrelation parameters between the last two observations in $\mathcal{I}_2$ (see Subsection 3.1). Furthermore, by comparing these power values to that at $\widehat{\tau}_1$, it is evident that they are significantly lower, leading us to classify this change as a false alarm.

Power	τ_1			
	90	110	150	195
$\widehat{\tau}_1$	90	110	150	195
$\mathcal{P}_{1,\widehat{\tau}_1-1}$	0.05099	0.05124	0.05091	0.05071
$\mathcal{P}_{1,\widehat{\tau}_1}$	0.05612	0.05721	0.05851	0.05762
$\mathcal{P}_{1,\widehat{\tau}_1+1}$	0.05218	0.05181	0.05213	0.05213
$\mathcal{P}_{1,\widehat{\tau}_1+2}$	0.05232	0.05194	0.05273	0.05224
$\mathcal{P}_{1,\widehat{\tau}_1+3}$	0.05212	0.05174	0.05283	0.05211
$\mathcal{P}_{1,\widehat{\tau}_1+4}$	0.05234	0.05179	0.05255	0.05215

Table 1. Power of the test around τ_1 for $\zeta = 0.4\%$ and $\alpha = 5\%$.

In the same line, we consider the problem of detecting changes, estimating their locations and identifying their type. For that, we generate a data that present one single change-point and one single false alarm using the following particular case of

model (5)

$$\begin{cases} X_t = & \rho_{0,1} + \rho_{0,2} X_{t-1} + \varepsilon_t, & t = 1, \ldots, \tau_1 - 1, \\ X_t = & \rho_{0,1} + \dfrac{\beta_{1,1}}{\sqrt{n}} + \left(\rho_{0,2} + \dfrac{\beta_{1,2}}{\sqrt{n}}\right) X_{t-1} + \varepsilon_t, & t = \tau_1, \ldots, n \\ X_{\tau_2} = & \epsilon, & \tau_1 <<< \tau_2 < n, \end{cases}$$

where $(\varepsilon_t)_{t\geq 1}$ is a standard Gaussian white noise and ϵ is a Gaussian random variable with different parameters values.
For $n = 300$, $\rho_{0,1} = 0.2$, $\rho_{0,2} = 0.3$, $\beta_{1,1} = 5$, $\beta_{1,2} = -3$, $\epsilon \sim \mathcal{N}(-1, 2)$ and $\zeta = 0.25\%$. Figure 2 illustrates the behavior of the power when facing a change. Now, for $n = 300$, $\rho_{0,1} = 0.2$, $\rho_{0,2} = 0.3$, Table 2 shows the estimation of the break locations corresponding to different type and magnitudes of changes, and different values of ζ.

	$((\beta_{11}, \beta_{1,2}), (\tau_1, \tau_2), \epsilon \sim, \zeta))^\top$			
	$(1, 1)$	$(3, -2)$	$(5, -3)$	$(10, -6)$
	$(101, 200)$	$(101, 250)$	$(111, 280)$	$(91, 295)$
	$\mathcal{N}(1, 1)$	$\mathcal{N}(1, 2)$	$\mathcal{N}(-1, 2)$	$\mathcal{N}(2, 2)$
$\widehat{\tau}$ and power	0.15%	0.25%	0.25%	0.35%
$\widehat{\tau}_1$	102	101	111	91
$\widehat{\mathcal{P}}_{1,\tau_1-1}$	0.050541	0.050713	0.050811	0.050972
$\widehat{\mathcal{P}}_{1,\tau_1}$	0.052418	0.053712	0.054612	0.057321
$\widehat{\mathcal{P}}_{1,\tau_1+1}$	0.052503	0.053515	0.054874	0.057819
$\widehat{\mathcal{P}}_{1,\tau_1+2}$	0.052315	0.053821	0.054731	0.057643
$\widehat{\mathcal{P}}_{1,\tau_1+3}$	0.052517	0.053644	0.054912	0.057967
$\widehat{\mathcal{P}}_{1,\tau_1+4}$	0.052421	0.053553	0.054826	0.058042
$\widehat{\tau}_2$	200	250	280	295
$\widehat{\mathcal{P}}_{2,\tau_2-1}$	0.050912	0.050626	0.050963	0.050121
$\widehat{\mathcal{P}}_{2,\tau_2}$	0.052915	0.054261	0.053987	0.061092
$\widehat{\mathcal{P}}_{2,\tau_2+1}$	0.051981	0.051725	0.516471	0.051681
$\widehat{\mathcal{P}}_{2,\tau_2+2}$	0.051734	0.051628	0.051811	0.051874
$\widehat{\mathcal{P}}_{2,\tau_2+3}$	0.051413	0.051632	0.051736	0.051642
$\widehat{\mathcal{P}}_{2,\tau_2+4}$	0.051386	0.051589	0.051481	0.051328

Table 2. Power around changes detected in a class of AR(1) model.

One can see that the behavior of the calculated local power is different between the estimates changes and it is easy to distinguish between a false alarm and a true change-point using

4.2. Multiple change-points detection (k=3)

In this part, we consider the problem of detecting multiple change-points in class of non-linear models, such as AR(1)-ARCH(1) model which is a particular class of CHARN(1,1) models. We use the same values of the parameters used in [33] in order to compare the results, efficiency and accuracy between the results obtained by that algorithm and those obtained by the new one introduced in this paper. In addition, for each detecting change, we monitor the power calculated at some instants around

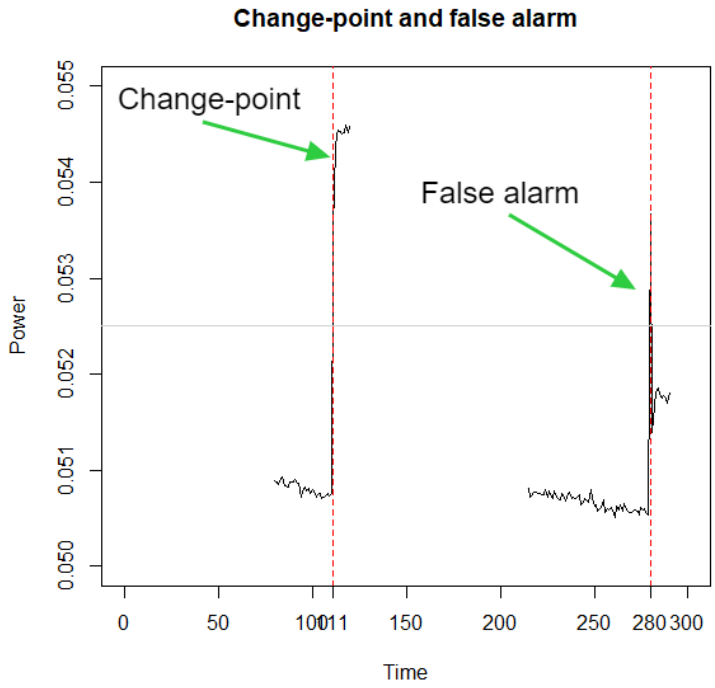

Figure 2. Behavior of the power when facing a change.

estimates instant of change in order to identify the type of the change detected. We consider the data generated by model (5), for $\tau = (\tau_1, \tau_2, \tau_3)$ represents the true instant of changes, $n = 350, \rho_{0,1} = 0.2$, $\rho_{0,2} = 0.3$, $\rho_{0,3} = \beta_{j,3} = 0$, $j = 1, 2, 3$, $\theta_1 = 1$, $\theta_2 = 0.02$. For 5000 replications, different magnitudes of change $\beta_j = (\beta_{j,1}, \beta_{j,2})$, $j = 1, 2, 3$ and same $\zeta = 0.1\%$, the results are shown on Table 3.

$\tau = (\tau_1, \tau_2, \tau_3) = (90, 190, 275)$									
				$\begin{pmatrix} \beta_{1,1} & \beta_{1,2} \\ \beta_{2,1} & \beta_{2,2} \\ \beta_{3,1} & \beta_{3,2} \end{pmatrix}$					
	$\begin{pmatrix} 3 & 2 \\ 1 & 3 \\ -1 & 1 \end{pmatrix}$			$\begin{pmatrix} 1 & -0.5 \\ 2 & 1 \\ -1 & -1 \end{pmatrix}$			$\begin{pmatrix} -2 & 1.5 \\ 1 & 3 \\ -0.5 & -1 \end{pmatrix}$		
i	$i = 1$	$i = 2$	$i = 3$	$i = 1$	$i = 2$	$i = 3$	$i = 1$	$i = 2$	$i = 3$
$\widehat{\tau}_i$	90	191	276	91	191	276	91	190	275
$\mathcal{P}_{i,\tau_i-1}$	0.050342	0.050314	0.050142	0.050214	0.050352	0.050324	0.050312	0.050963	0.050561
$\mathcal{P}_{i,\tau_i}$	0.052117	0.052203	0.052722	0.051917	0.052134	0.053341	0.052162	0.053102	0.053978
$\mathcal{P}_{i,\tau_i+1}$	0.052313	0.052491	0.052524	0.052023	0.052232	0.053242	0.052213	0.528902	0.538511
$\mathcal{P}_{i,\tau_i+2}$	0.052325	0.051908	0.052498	0.051976	0.052109	0.053234	0.051909	0.052932	0.053915
$\mathcal{P}_{i,\tau_i+3}$	0.052318	0.052424	0.052713	0.052014	0.052421	0.053517	0.052132	0.053011	0.053776
$\mathcal{P}_{i,\tau_i+4}$	0.052521	0.052510	0.052613	0.052134	0.051996	0.053127	0.052193	0.053106	0.053817

Table 3. Power around changes detected in a class of AR(1)-ARCH(1) model.

One can see from Table 3 that the results is more accurate than those obtained in [33], for example, for $\beta = ((3, 1, -1), (2, 3, 1))^\top$, the estimated change points in [33] are $(93, 193, 277)$. The results we obtain here are more accurate.. In addition, for a suitable threshold corresponding to a suitable ζ, it is rarely that we find a detection

change in advance of the real instant of break from which it was removed during the replications. This feature is a result of the newly introduced algorithm here, which reduces the impact of white noise.

5. Real dataset

In this section, we apply our approach to real-world datasets from two different fields. First, we examine the industrial sector by analyzing welding electrical signals recorded during arc welding. Then, we turn to the financial sector, applying our method to two major market indices: the S&P 500 and FTSE 100. We also demonstrate the effectiveness of our approach in detecting changes that have not been identified in previous studies, highlighting its robustness and sensitivity in diverse applications.

5.1. Welding electrical signals

5.1.1. Introduction

Welding is a critical process for many industries, particularly those involved in the construction of hot water tanks. Detecting and locating faults in welds is essential for quality control. Welding electrical signals (WES) are widely used as a data source for fault detection, with numerous studies addressing this issue. For instance, [19] detected three types of welding defects using a Support Vector Machine (SVM) model based on the multi-scale entropy of current and voltage signals. Similarly, [28] classified sound signals to detect shielding gas absence with an Artificial Neural Network. From a time series perspective, [25] proposed a method for defect detection and localization based on causality analysis, following the foundational work of [20] on time series causality.

In arc welding, changes in the mean of WES are often caused by variations in the distance between the electrode and the surface being welded, which may indicate irregularities in the metal surface. These variations can result from faults during metal plate transformation or the presence of holes in the material.

Our primary goal is to test for weak changes in the mean of arc welding series, which are considered "normal welding series," to monitor the stability of the electrical signals. The data used in this study were provided by the Leblanc company, consisting of 10 normal weld experiments conducted under identical conditions. We analyze all of these datasets, presenting results from four of them.

5.1.2. Modeling and results

First, we start our study by looking for a common suitable time series model for all of these data. The chronogram of the WES series (W_t) seems to present a trend and does not present a seasonality. The Augmented Dicky-Fuller test (see [7]) approve the non-stationarity of all these data. The results obtained in [33] cannot be used directly, since the Moving-Average part doesn't belongs to the class of CHARN models used there. For that, we decompose these series in a summation of two components as follow:

$$W_t = Y_t + X_t,$$

where (Y_t) represents the unknown trend assumed to be continuous and (X_t) is a piecewise stationary series with mean (μ_t) and variance (σ_t). The time interval between capturing each signal in the time series is 0.1 seconds. To consider the whole (the smallest thing we want to detect its impact) in the surface significant, at least 5 signals must be recorded. So, we estimate the trend by the following moving-average with order 5

$$\widehat{Y}_t = \frac{1}{5}\sum_{j=-2}^{2} W_{t+j}.$$

Now, we apply the algorithm presented in Section 3.2 to the series X_t of the first data that we have, where we consider $m = 25$, and $\iota = 300$. Table 4 shows the most frequent models obtained.

Model	Frequency
ARIMA(0,0,0)	281
ARIMA(1,0,0)	3
ARIMA(1,0,1)	2

Table 4. The most frequently selected CHARN models for the welding electrical signals.

We apply this technique on the other data, and approximately, same results have been obtained. Then, we propose the following model

$$X_t = \rho_{0,1} + \frac{\beta_{j,1}}{\sqrt{n}} + \sigma_j \varepsilon_t, \quad t \in [\tau_{j-1}, \tau_j), \quad j = 1, \ldots, k+1,$$

where k is the number of change-points that assumed to be unknown and must be estimated, $\tau_1, \ldots, \tau_k$ designate the breaks locations, (ε_t) is a standard Gaussian white noise, $V(x) = \sigma_j$ represents the variance of X_t in each interval $[\tau_{j-1}, \tau_j)$.
Here, for the test problem, $\boldsymbol{\gamma}_0 = 0$, $\boldsymbol{\gamma}_n = (0, \beta_2/\sqrt{n}, \ldots, \beta_{k+1}/\sqrt{n}) \in \mathbb{R}^{k+1}$ with $\boldsymbol{\beta} = (0, \beta_2, \ldots, \beta_{k+1})$.
Using the theoretical results of [33] recalled in Section 2, and by applying our algorithm presented in Subsection 3.1, for different thresholds corresponding to the choice of ζ, we detect multiple breaks in the data and we show the results of 4 of them for $\zeta = 0.15\%$, 0.25%, and 0.3% on Figures 3 to 14.

Now, since all of these data are considered as a normal welding, it is interesting to take a look to the variation of the number of changes detected with respect to the threshold. For that, we consider a sequence of ζ varying between 0.15% and 1%, we applied our algorithm on each data for each value of ζ and we calculate the corresponding number of changes detected. The results are shown on Figure 15.

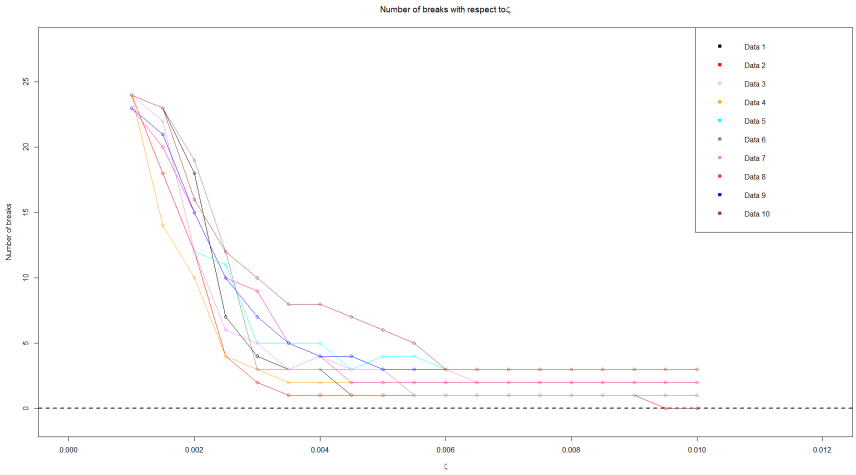

Figure 15. Number of breaks with respect to ζ.

5.1.3. Analyses

For these 10 data, we applied our algorithm for ζ varying between 0.1% and 1%. For $0.1\% \leq \zeta \leq 0.13\%$, a high number of weak breaks has been detected which is not an informative phenomenon in this domain. Figure 3 to 14 shows the corresponding breaks detected of four of these data for $\zeta = 0.15\%$, 0.25% and 0.3%. It is easy to see that the number of changes detected decrease when the threshold increase which is logic, and also, some estimated breaks locations remains close to each other even when varying the threshold. For example, in Data 2, the instant $t = 589$ remains the same instant detected when $\zeta = 0.15\%$ or 0.3%. This is caused by the magnitude of the power from which it remains high then these threshold. For that, we can consider it as a true change.

Also, for all of these data, when a change is detected, the power remains above the threshold except the case of that corresponding to Data 2 where, for $\zeta = 0.25\%$, 0.3%, the instant $t = 2245$ is considered as a false alarm and it can be explained here by a hole in the surface plate under welds.

These results allows us to assume the segmentation of the data into piece-wise stationary data from which the distance between the observations that belong to every single piece and the electrode is significantly constant. One can see that, by fixing a threshold, we can find the reason that make the distance between the electrode and the surface metal plat under welds change. By monitoring the values of the power of the test, we can classify the changes detected into a deformation of the circular form of the hot water tank or a hole. In other word, the false alarm definition introduced in Subsection 3.1 can be explained here as a hole from which the power cross the threshold for a few number of observations, and the true change as the point where the deformation of the circular form started.

From Figure 15, we can see that the number of breaks detected decrease exponentially when ζ varying between 0.15% and 0.35% and then, it remains constant for a while before converging to zero. We can explain this fall of the number of changes detected through the small magnitude of changes and the weak variation of the values of the welding signals from which the power of the test cross the threshold for a small ζ and it remains under the threshold for a higher ζ. In addition, by taking $\zeta = 9\%$, no change has been detected in all of these data.

5.2. Financial data

5.2.1. Standard & Poor's 500 Index (S&P 500)

Here, we apply our newly our approach to financial data, specifically the S&P 500 index's daily stock prices. We utilize daily data from January 1992 to December 2000, the same dataset used in [33], to determine whether the new algorithm detects subtle changes that may have gone undetected by the previously proposed algorithm.

Since the data exhibits a trend indicating that the S&P 500 index is non-stationary, we work with the transformed series X_t, defined as:

$$X_t = \log\left(\frac{P_t}{P_{t-1}}\right),$$

where P_t represents the S&P 500 price index at time t. This transformation ensures that any potential breaks in the series P_t are preserved in X_t, due to the continuity property of the logarithmic function.

As described in Subsection 3.1, we begin by assuming stationarity over m observations, where we set $m = 25$ based on the approximate number of trading days in a month. Additionally, we consider a vector of 200 different random variables u $(h = 200)$, $u \in U[1, n - m = 2020 - 25]$, representing randomly selected sub-samples from the dataset.

Next, to identify the most suitable CHARN model, we implement our algorithm presented in Section 3.2. The dominant repetitive model is summarized in Table 5.

Model	Frequency
ARIMA(0,0,0)	166
ARIMA(1,0,0)	5
ARIMA(2,0,0)	2

Table 5. The most frequently selected particular CHARN models for S&P 500 Index.

Finally, using our methodology, we adopt the same model proposed in [33], which is defined as follows:

$$X_t = \frac{\beta_j}{\sqrt{n}} + \theta_j \varepsilon_t, \quad t \in [\tau_j, \tau_{j+1}[, \quad \varepsilon_t \sim N(0,1),$$

where β_j and θ_j represent the model parameters, and ε_t is a standard normally distributed error term. Then, applying our algorithm for changes detection using this model, we detects the changes presented in this series and explained with Figure 16.

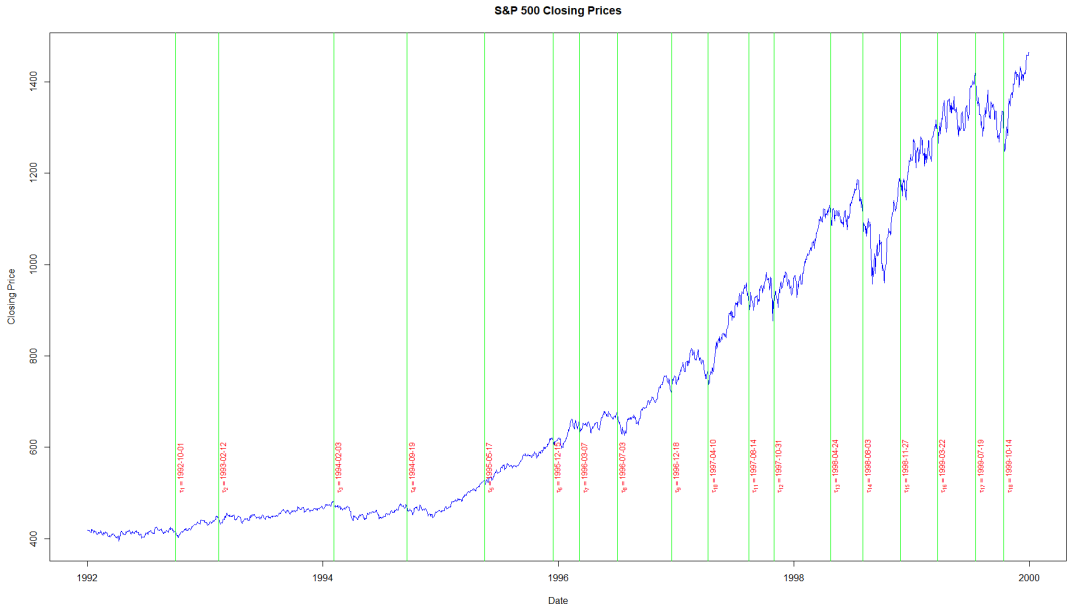

Figure 16. Estimated breaks detected in S&P 500 indices.

While the old algorithm successfully identified several significant changes in the S&P 500 index, the new algorithm detects additional important breaks that correspond to events not captured by the previous technique.

For instance, the new algorithm identified **1993-02-12**, a change point which could be linked to the inauguration of President Bill Clinton and the anticipation surrounding his economic policies aimed at reducing the federal deficit. This period marked the beginning of shifts in fiscal policy, which could explain the market's response. However, this subtle change was not captured by the old algorithm.

Similarly, the date **1994-09-19**, identified by the new algorithm, corresponds to the bond market crisis, also known as the "Bond Market Massacre" of 1994. The old algorithm identified a related point in **1994-03-03**, which we linked to the U.S. lifting of the trade embargo on Vietnam, but failed to capture the subsequent market turbulence later in the year.

Moreover, the new algorithm detects **1997-04-10**, which likely reflects the market's reaction to early concerns about inflation and potential interest rate hikes. This date is not detected by the previous algorithm, which only identified **1997-07-14**, likely driven by the deepening Asian financial crisis.

Another example is the detection of **1996-03-07**, a subtle change linked to the Federal Reserve's decision to hold interest rates steady after prior hikes. This change was missed by the old algorithm, which only captured a later date in July 1996 (**1996-07-11**), possibly linked to strong corporate earnings at the time.

Additionally, the new algorithm identifies **1998-08-03**, coinciding with the start of the Russian financial crisis, whereas the old algorithm only captured **1998-06-22** and **1998-11-02**, which were connected to market reactions to the Long-Term Capital Management (LTCM) crisis and the Federal Reserve's rescue operation.

An important remark must be made regarding the dates 1997-04-10 and 1997-07-19, when the estimated local power crossed the threshold, signaling the presence of

a critical point. It subsequently fell below the threshold after 4 and 5 observations, respectively. The technique we use to achieve this is detailed in the algorithm described in Subsection 3.1.Additionally, we can conclude that, in real-world data, the events occurring at these times had a distinct, short-term impact, unlike those that caused more persistent changes at other dates.

In conclusion, the new algorithm not only confirms several change points identified by the old method but also detects additional, earlier, or subtler changes linked to significant market events. This enhancement demonstrates the improved sensitivity of the new algorithm in capturing weak changes in financial markets that the previous algorithm overlooked.

5.2.2. Financial Times Stock Exchange 100 Index (FTSE 100)

In this part, we apply our approach to detects the change in the FTSE 100 index. We use daily data from July 27th, 2005, to July 13th, 2009. Instead of using the original data where the trend appears clearly, we use the logarithm return as defined in the previous section. As we explain in the previous section, we begin by assuming the stationarity of the first m observations, where we set again $m = 25$ based on approximate number of trading days in a month. Using the same values and following the same procedure as in the previous section, the dominant repetitive model among 300 subset considered is summarized in the Table 6.

Model	Frequency
ARIMA(0,0,0)	226
ARIMA(0,1,0)	11
ARIMA(1,0,0)	16
ARIMA(3,0,0)	13

Table 6. The most frequently selected particular CHARN models for a subset of FTSE 100 Index.

Out of 300 subsets derived from the original dataset of 1004 observations, 16 subsets suggest an Autoregressive AR(1) model, indicating that the daily price depends on the previous day's price value. Additionally, 13 subsets suggest that the price depends on the price values from the past three days. However, the dominant model identified is the shifted model, which consists of a mean plus an error term. This shifted model will be the one utilized for further analysis. Using these results, we adjust the following particular CHARN model

$$X_t = \frac{\beta_j}{\sqrt{n}} + \theta_j \varepsilon_t, \quad t \in [\tau_j, \tau_{j+1}[, \quad \varepsilon_t \sim N(0,1),$$

where β_j and θ_j represent the model parameters, and ε_t is a standard normally distributed error term. By applying our change detection algorithm using this model, we successfully identified the structural changes present in the series, as illustrated in Figure 17.

Figure 17. Estimated breaks detected in FTSE 100 Index.

[13] proposed a technique for detecting changes, referred to as the BASTA-res technique, which the authors applied to the FTSE 100 index over the same period analyzed here. The corresponding dates detected by their method are notably June 5, 2007, August 18, 2008, and December 4, 2008. These dates align with significant financial events, such as the onset of the subprime mortgage crisis and the collapse of Lehman Brothers. While their method successfully identifies these key turning points, our approach provides additional insights by detecting earlier and intermediate structural changes, such as on February 26, 2007, and July 25, 2007, indicating shifts in market dynamics preceding the financial crisis.

For instance, the change point on May 11, 2006, detected by our algorithm, likely reflects global market concerns about inflation and interest rates, which triggered a broader sell-off. Similarly, the change point on July 25, 2007, reflects early signs of market volatility linked to the subprime crisis, a significant moment that went undetected by [13]. Furthermore, our algorithm detected important changes on January 18, 2008, March 20, 2008, and September 18, 2008, providing a more detailed representation of market turbulence during the 2008 financial crisis.

These additional change points underscore the increased sensitivity and granularity of our approach. By identifying earlier and more frequent structural changes, it offers a deeper understanding of the market's evolving behavior, which could be crucial for more proactive risk management. The results demonstrate that our approach not only captures major financial disruptions, as found by [13], but also identifies critical early warning signals and minor shifts, providing a more comprehensive view of the market's volatility."

6. Conclusion

We have introduced a new automatic algorithm for detecting subtle changes in the mean, building on the method proposed by [33]. Additionally, we have presented a complementary technique to help select the appropriate model for change detection. The simulation experiments demonstrate that our algorithm is effective in detecting multiple breaks and distinguishing between true change points and false alarms. Compared to the results obtained in [33], our algorithm appears to be more efficient and accurate, offering an additional technique of significant value when applied to real-world data. This was evident in how it captured the impact of specific events on financial data.
By applying the theoretical results of [33] with the algorithm proposed here, we detect multiple weak changes in the welding electrical signals in order to study the stability of the electrical tension during the construction of hot water tank and identifying the reason about these changes.
Furthermore, the application of our approach to financial datasets demonstrates its effectiveness in detecting changes driven by significant events impacting these indices. Compared to results from other studies, our approach not only accurately identifies the same points of change but also uncovers additional changes that were missed by other methods. These newly detected changes can be linked to specific events, further validating the robustness and precision of our algorithm in capturing subtle shifts in the data.
A key perspective of our approach in this study involves developing an automated method to determine the optimal threshold for the specific domain under investigation. Addressing this global challenge is a paramount concern for numerous researchers in this field, and it stands as a significant focus for our forthcoming endeavors.

Acknowledgement(s)

Authors would like to thank Abdallah Amine Melakhsou and elm.leblanc France (www.elmleblanc.fr), for providing the real data used in this paper.

Disclosure statement

The authors declare no conflicts of interest

Funding

This research received no external funding.

Notes on contributor(s)

Conceptualization, Y.S.; methodology, Y.S., A.H. and M.B.-H.; software, Y.S.; validation, Y.S., A.H. and M.B.-H.; formal analysis, Y.S. and A.H.; data collection and pretreatment, Y.S. and A.H.; writing—original draft preparation, Y.S.; writing—review

and editing, Y.S., A.H. and M.B.-H. All authors have read and agreed to the published version of the manuscript.

References

[1] Andreou, E. and Ghysels, E. (2009). Structural breaks in financial time series. *Handbook of financial time series*, pages 839–870.

[2] Aue, A. and Horváth, L. (2013). Structural breaks in time series. *Journal of Time Series Analysis*, 34(1):1–16.

[3] Beaulieu, C., Chen, J., and Sarmiento, J. L. (2012). Change-point analysis as a tool to detect abrupt climate variations. *Philosophical Transactions of the Royal Society A: Mathematical, Physical and Engineering Sciences*, 370(1962):1228–1249.

[4] Brockwell, P., Davis, R., and Salehi, H. (1990). A state-space approach to transfer-function modeling. *Statistical Inference in Stochastic Processes*, 6:233.

[5] Brown, R. L., Durbin, J., and Evans, J. M. (1975). Techniques for testing the constancy of regression relationships over time. *Journal of the Royal Statistical Society: Series B (Methodological)*, 37(2):149–163.

[6] Chen, G.-y., Gan, M., and Chen, G.-l. (2018). Generalized exponential autoregressive models for nonlinear time series: stationarity, estimation and applications. *Information Sciences*, 438:46–57.

[7] Cheung, Y.-W. and Lai, K. S. (1995). Lag order and critical values of the augmented dickey–fuller test. *Journal of Business & Economic Statistics*, 13(3):277–280.

[8] Cho, H. and Fryzlewicz, P. (2012). Multiscale and multilevel technique for consistent segmentation of nonstationary time series. *Statistica Sinica*, pages 207–229.

[9] Davis, R. A., Lee, T. C. M., and Rodriguez-Yam, G. A. (2006). Structural break estimation for nonstationary time series models. *Journal of the American Statistical Association*, 101(473):223–239.

[10] Diop, M. L. and Kengne, W. (2023). A general procedure for change-point detection in multivariate time series. *TEST*, 32(1):1–33.

[11] Droesbeke and Fine, J.-J. (1996). *Inférence non paramétrique: Les statistiques de rangs*. Ed. de l'Université de Bruxelles; Ed. Ellipses.

[12] Fryzlewicz, P. (2014). Wild binary segmentation for multiple change-point detection. *The Annals of Statistics*, 42(6):2243–2281.

[13] Fryzlewicz, P. and Subba Rao, S. (2014). Multiple-change-point detection for auto-regressive conditional heteroscedastic processes. *Journal of the Royal Statistical Society Series B: Statistical Methodology*, 76(5):903–924.

[14] Hadj-Amar, B., Rand, B. F., Fiecas, M., Lévi, F., and Huckstepp, R. (2020). Bayesian model search for nonstationary periodic time series. *Journal of the American Statistical Association*, 115(531):1320–1335.

[15] Hallgren, K. L., Heard, N. A., and Adams, N. M. (2022). Changepoint detection in non-exchangeable data. *Statistics and Computing*, 32(6):110.

[16] Härdle, W., Tsybakov, A., and Yang, L. (1998). Nonparametric vector autoregression. *Journal of Statistical Planning and Inference*, 68(2):221–245.

[17] Horváth, L. (1993). The maximum likelihood method for testing changes in the parameters of normal observations. *The Annals of statistics*, pages 671–680.

[18] Horváth, L., Miller, C., and Rice, G. (2020). A new class of change point test statistics of rényi type. *Journal of Business & Economic Statistics*, 38(3):570–579.

[19] Huang, Y., Yang, D., Wang, K., Wang, L., and Zhou, Q. (2020). Stability analysis of gmaw based on multi-scale entropy and genetic optimized support vector machine. *Measurement*, 151:107282.

[20] Kamiński, M., Ding, M., Truccolo, W. A., and Bressler, S. L. (2001). Evaluating causal relations in neural systems: Granger causality, directed transfer function and statistical assessment of significance. *Biological cybernetics*, 85:145–157.

[21] Killick, R., Fearnhead, P., and Eckley, I. A. (2012). Optimal detection of changepoints with a linear computational cost. *Journal of the American Statistical Association*, 107(500):1590–1598.

[22] Korkas, K. K. and PryzlewiczV, P. (2017). Multiple change-point detection for non-stationary time series using wild binary segmentation. *Statistica Sinica*, pages 287–311.

[23] Le Cam, L. (1986). The central limit theorem around 1935. *Statistical science*, pages 78–91.

[24] Ltaifa, M. (2021). *Tests optimaux pour détecter les signaux faibles dans les séries chronologiques*. Theses, Université de Lorraine ; Université de Sousse (Tunisie).

[25] Melakhsou, A. A. and Batton-Hubert, M. (2021). On welding defect detection and causalities between welding signals. In *2021 IEEE 17th International Conference on Automation Science and Engineering (CASE)*, pages 401–408. IEEE.

[26] Ngatchou-Wandji, J. and Ltaifa, M. (2023). Detecting weak changes in the mean of a class of nonlinear heteroscedastic models. *Communications in Statistics - Simulation and Computation*, 0(0):1–33.

[27] Page, E. S. (1954). Continuous inspection schemes. *Biometrika*, 41(1/2):100–115.

[28] Pernambuco, B. S. G., Steffens, C. R., Pereira, J. R., Werhli, A. V., Azzolin, R. Z., and Estrada, E. d. S. D. (2019). Online sound based arc-welding defect detection using artificial neural networks. In *2019 Latin American robotics symposium (LARS), 2019 Brazilian symposium on robotics (SBR) and 2019 workshop on robotics in education (WRE)*, pages 263–268. IEEE.

[29] Perron, P. et al. (2006). Dealing with structural breaks. *Palgrave handbook of econometrics*, 1(2):278–352.

[30] Reeves, J., Chen, J., Wang, X. L., Lund, R., and Lu, Q. Q. (2007). A review and comparison of changepoint detection techniques for climate data. *Journal of applied meteorology and climatology*, 46(6):900–915.

[31] Salman, Y. (2022). *Testing a class of time-varying coefficients CHARN models with application to change-point study*. PhD thesis, Lorraine University; Lebanese University.

[32] Salman, Y., Hoayek, A., and Batton-Hubert, M. (2024a). New algorithm for detecting weak changes in the mean in a class of charn models with application to welding electrical signals. *Engineering Proceedings*, 68(1):42.

[33] Salman, Y., Ngatchou-Wandji, J., and Khraibani, Z. (2024b). Testing a class of piece-wise charn models with application to change-point study. *Mathematics*, 12(13):2092.

[34] Stoumbos, Z. G., Reynolds Jr, M. R., Ryan, T. P., and Woodall, W. H. (2000). The state of statistical process control as we proceed into the 21st century. *Journal of the American Statistical Association*, 95(451):992–998.

[35] Vostrikova, L. Y. (1981). Detecting "disorder" in multidimensional random processes. In *Doklady akademii nauk*, volume 259, pages 270–274. Russian Academy of Sciences.

[36] Yao, Y.-C. (1987). Approximating the distribution of the maximum likelihood estimate of the change-point in a sequence of independent random variables. *The Annals of Statistics*, pages 1321–1328.

[37] Yau, C. Y. and Zhao, Z. (2016). Inference for multiple change points in time series via likelihood ratio scan statistics. *Journal of the Royal Statistical Society: Series B (Statistical Methodology)*, 78(4):895–916.

[38] Zeileis, A. (2001). p values and alternative boundaries for cusum tests. Technical report, Technical Report.

[39] Zeileis, A. (2004). Alternative boundaries for cusum tests. *Statistical Papers*, 45(1):123–131.

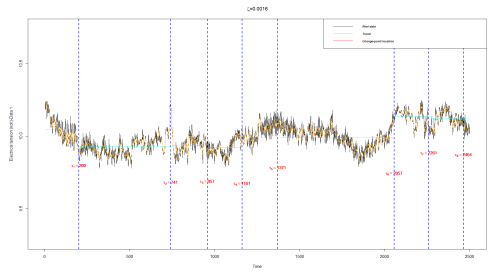

Figure 3. Data 1 and $\zeta = 0.15\%$.

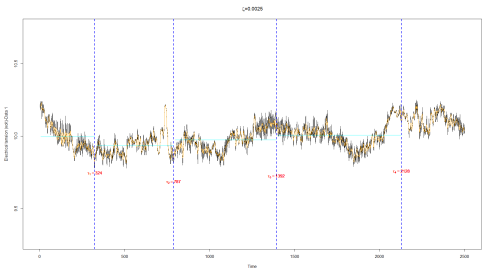

Figure 4. Data 1 and $\zeta = 0.25\%$.

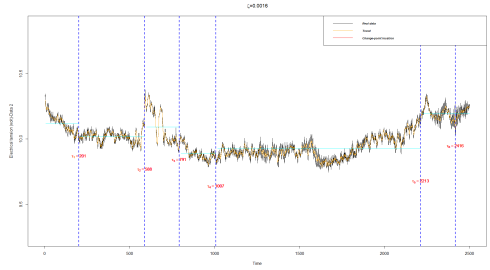

Figure 5. Data 2 and $\zeta = 0.15\%$.

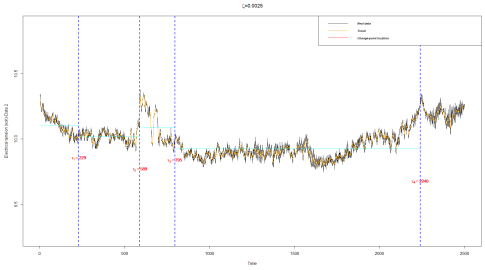

Figure 6. Data 2 and $\zeta = 0.25\%$.

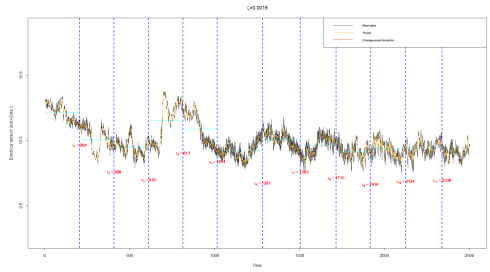

Figure 7. Data 3 and $\zeta = 0.15\%$.

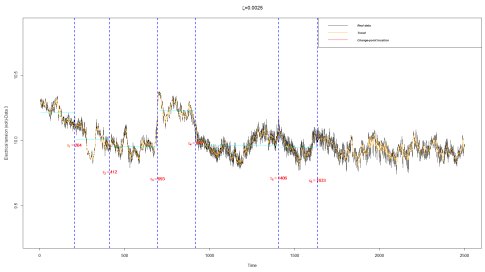

Figure 8. Data 3 and $\zeta = 0.25\%$.

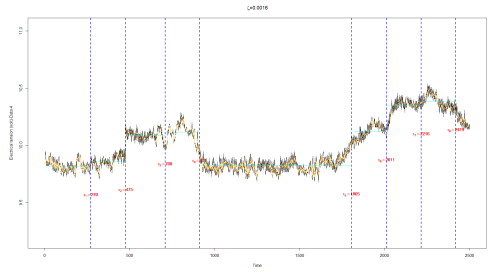

Figure 9. Data 4 and $\zeta = 0.15\%$.

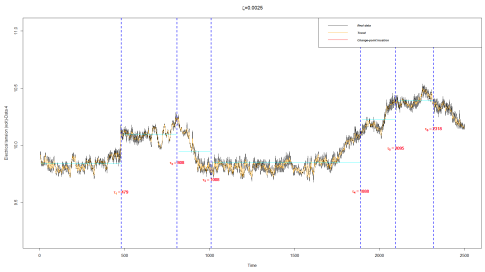

Figure 10. Data 4 and $\zeta = 0.25\%$.

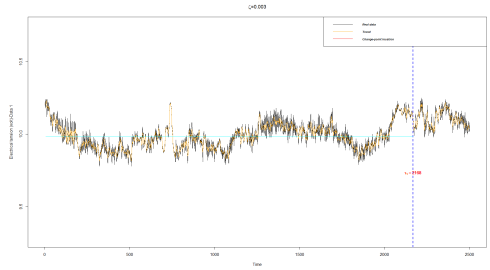

Figure 11. Data 1 and $\zeta = 0.3\%$.

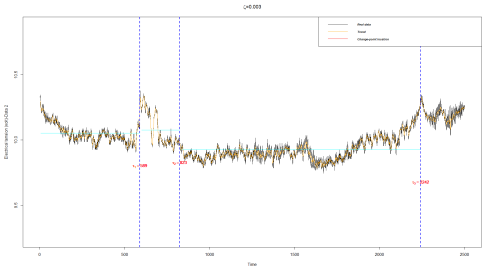

Figure 12. Data 2 and $\zeta = 0.3\%$.

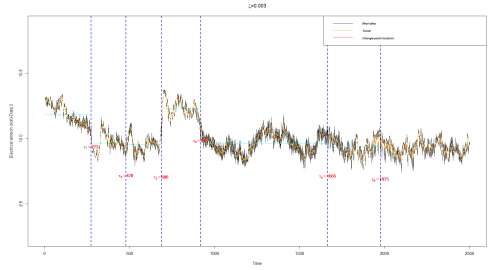

Figure 13. Data 3 and $\zeta = 0.3\%$.

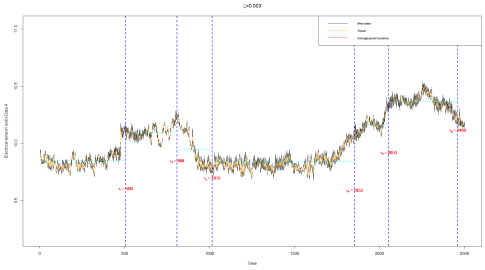

Figure 14. Data 4 and $\zeta = 0.3\%$.